

Dispersion stability of nanoparticles in ecotoxicological investigations: the need for adequate measurement tools

Ratna Tantra · Shingheng Jing ·
Sivaraman K. Pichaimuthu · Nicholas Walker ·
James Noble · Vincent A. Hackley

Received: 20 October 2010 / Accepted: 14 February 2011
© Crown Copyright 2011

Abstract One of the main challenges in nanoecotoxicological investigations is in the selection of the most suitable measurement methods and protocols for nanoparticle characterisation. Several parameters have been identified as being important as they govern nanotoxicological activity, with some parameters being better defined than others. For example, as a parameter, there is some ambiguity as to how to measure dispersion stability in the context of ecotoxicological investigations; indeed, there is disagreement over which are the best methods to measure nanoparticle dispersion stability. The purpose of this article is to use various commercially available tools to measure dispersion stability and to understand the information given by each tool. In this study, CeO₂ was dispersed in two different types of media: de-ionised water and electrolyte-containing fish medium. The DLS mean particle size of freshly dispersed sample in DI water was ~200 nm in diameter. A visual sedimentation experiment showed

that nanoparticle dispersion made in the fish medium was less stable compared to corresponding dispersion in de-ionised water. Stability of these dispersions was monitored using various techniques, for a period of 3 days. Our findings have shown that dispersion stability can be suitably assessed by monitoring: (a) surface charge, (b) sedimentation events and (c) presence of agglomerates, through time. The majority of techniques employed here (zeta potential, particle size via DLS, fluorescence and UV–Vis spectroscopy and SEM) were shown to provide useful, complementary information on dispersion stability. Nanoparticle Tracking Analysis (NTA) provides useful, quantitative information on the concentration of nanoparticles in suspension, but is limited by its inability to accurately track the motion of large agglomerates found in the fish medium.

Keywords Nanoparticles · Dispersions · Nanomaterial characterisation · Nanometrology · Environmental and health effects

R. Tantra (✉) · S. Jing · S. K. Pichaimuthu · J. Noble
National Physical Laboratory, Hampton Road,
Teddington, Middlesex TW11 0LW, UK
e-mail: ratna.tantra@npl.co.uk

N. Walker
School of Biosciences, University of Exeter,
Geoffrey Pope Building, Exeter EX4 4QD, UK

V. A. Hackley
National Institute of Standards and Technology, 100
Bureau Drive, Gaithersburg, MD 20899-8520, USA

Introduction

The potential toxicity of nanoparticles has attracted attention in recent years and consequently has presented a dilemma to toxicologists and risk assessors in general (Boverhof and David 2010). The main research bottleneck is in the ability to reliably link

bioassay data with the relevant physicochemical properties of the nanoparticle preparations. This in turn is governed by the lack of agreed, validated protocols for the evaluation of nanoparticle toxicity (Tiede et al. 2008). A significant hurdle, in the case of physicochemical characterisation tests, is the lack of suitable tools to measure, low concentrations of nanoparticles (ng/L or less) reliably in complex media (Simonet and Valcarcel 2009). This requires techniques that can offer: sensitivity, high selectivity, and ‘representativeness’ of the entire sample population. Due to the lack of suitable tools, past researchers such as Powers et al. (Powers et al. 2006) have put forward a strategy ‘to characterise with as many methods as possible’; in doing so, researchers are allowed to ‘pick and choose’ on what or how to perform the characterisation step. In reality, different tools yield different information and their accuracy will be very much dependent on the strengths and limitations of the individual techniques. For example, it is known that for the measurement of particle size, dynamic light scattering (DLS) will give a different answer relative to imaging-based techniques such as atomic force microscopy (AFM); this difference is linked with sample preparation issues and with dry versus wet measurements. An excellent example of these apparent size discrepancies can be found in the report of analysis for NIST reference material 8012 (gold nanoparticles, nominally 30 nm) (Reference Material 8012—Gold Nanoparticles), which was characterised by six independent sizing methods; the reported reference values for DLS and AFM are consistently different, with DLS typically larger compared with AFM and other microscopy methods.

The objective of this study is to further explore the impact of using different tools to measure other parameters. In particular, we are interested to study those parameters, whose importance may be widely recognised, but which have no defined guidelines for the best methods/tools to use for their measurement. In the nanoeotoxicological context, ‘dispersion stability’ is an important parameter, as this relates to the assessment of fate, exposure and subsequent bioavailability (thus biological effect); in general, the more stable the dispersion, the higher the bioavailability. In the past, researchers have equated this parameter to the monitoring of particle size change through time (agglomerate formation) and corresponding zeta-potential measurements (Handy et al.

2008). Others have also equated this to indicate the level of ‘resistance to sedimentation’ and coagulation (or flocculation), which can be expressed as the ‘constancy of the number of particles per unit volume’ in the dispersion (Kissa 1999). If the dispersion is unstable, then we expect: (a) lower zeta-potential values (irrespective of polarity), (b) increase in particle size with time as particles agglomerate and (c) decrease in particle concentration with time in the upper dispersion layer as larger agglomerates sediment out.

The main question put forward in this study is: ‘Do different methods lead to different results and, if so, to what extent do they impact the final interpretation of the state of dispersion?’ To address this question, CeO₂ (an industrially relevant nanoparticle) is dispersed in both deionized (DI) water and fish medium; in the past, the dispersion of CeO₂ nanoparticles in DI water at concentrations of 50 mg/L or less, was shown to be stable after a period of 3 days. We will assess the state of dispersion through the use of various measurement techniques, viz.: visual inspection of sedimentation, UV–Vis and fluorescence spectroscopy, DLS, scanning electron microscopy (SEM), zeta-potential measurements (microelectrophoresis) and nanoparticle tracking analysis (NTA).

The media analysed was selected based on previous studies highlighting the differences in stability between DI water and fish medium, thereby providing a good model for comparison.

Tools were chosen on the basis that they are: (a) commercially available, and (b) the measurand is different. Out of all the techniques employed here, NTA is considered a relative newcomer to the nanoparticle analysis toolkit. NTA technology has the capability to measure particle size and number concentration in situ; particle size measurement involves tracking the Brownian motion of individual particles using a digital camera and tracking software (Malloy and Carr 2006). As with DLS, the hydrodynamic size of the particle is reported, calculated through the Stokes–Einstein equation. Although NTA is a relatively new technique with limited validation data (Filipe et al. 2010), we have selected this method as it is less sensitive than DLS to signal domination by larger particles and offers some complementary information, such as particle number concentration, unattainable from the other methods used in this study.

Experimental details

Materials

Nanocrystalline cubic CeO₂ powder (NanoGrain CeO₂ CMP, 99.95 %) ¹ was obtained from Umicore (Olen, Belgium). The manufacturer specifies a median particle size of (70 ± 11) nm for particles dispersed in water after 24 h and based on an X-ray disc centrifuge (XDC) method. The Brunauer–Emmett–Teller—commonly called BET—specific surface area is specified as (30 ± 3) m²/g. The supplier also specifies an isoelectric point (IEP) of 8.5 ± 0.5. The primary particles in suspension appear to exist as small compact aggregates of primary crystallites.

The CeO₂ particles were dispersed in one of two aqueous media: de-ionised (DI) water and fish medium at pH 7.0, as measured according to guidelines in ISO-7346/3 (1996). The composition of the fish medium is presented in Table 1, with salts obtained from Sigma-Aldrich, UK.

Nanoparticle powders (50 mg) were weighed, using an analytical mass balance, into clean glass vials. A few drops of the appropriate liquid medium were added to each individual vial and mixed into a thick paste using a spatula. Approximately 15 mL of liquid media was then added to the paste and the whole mixture gently stirred using a spatula. A de-agglomeration step was then carried out by using an ultrasonic probe (130 W, Ultrasonic Processors, Cole-Palmer, UK), with a probe tip (6 mm diameter Ti tip) that was inserted to the half way point between the surface and the bottom of the 15 mL suspension volume. The sample was then sonicated at 90% amplitude for 20 s; temperature measurements were made using a digital thermometer (Fisher Scientific) before and after the sonication step, and showed a temperature increase of ≈ 5 °C in the dispersion. The increase in temperature coincides with findings as reported previously (Tantra et al. 2010). After sonication, the nanoparticle suspension was diluted using the appropriate liquid medium to a 1-L total

¹ Certain trade names and company products are mentioned in the text or identified in illustrations in order to specify adequately the experimental procedure and equipment used. In no case does such identification imply recommendation or endorsement by National Institute of Standards and Technology, nor does it imply that the products are necessarily the best available for the purpose.

Table 1 Nanoparticle dispersion and analysis

	Chemical formula	Concentration mmol/L
Calcium chloride	CaCl ₂	4.87
Magnesium sulphate	MgSO ₄	1.92
Sodium bicarbonate	NaHCO ₃	1.54
Potassium chloride	KCl	0.15

volume with a final nanoparticle concentration of 50 mg/L. In order to ensure homogeneity, a glass rod was used to gently mix the final dispersion. Dispersions were stored in a separate pre-cleaned 1 L media glass bottle. Optical images showing the state of the dispersion in the bottles were recorded using a digital camera at set intervals over the analysis period of 3 days. Sample bottles were stored in the dark, when images were obtained care was taken not to disturb the suspension.

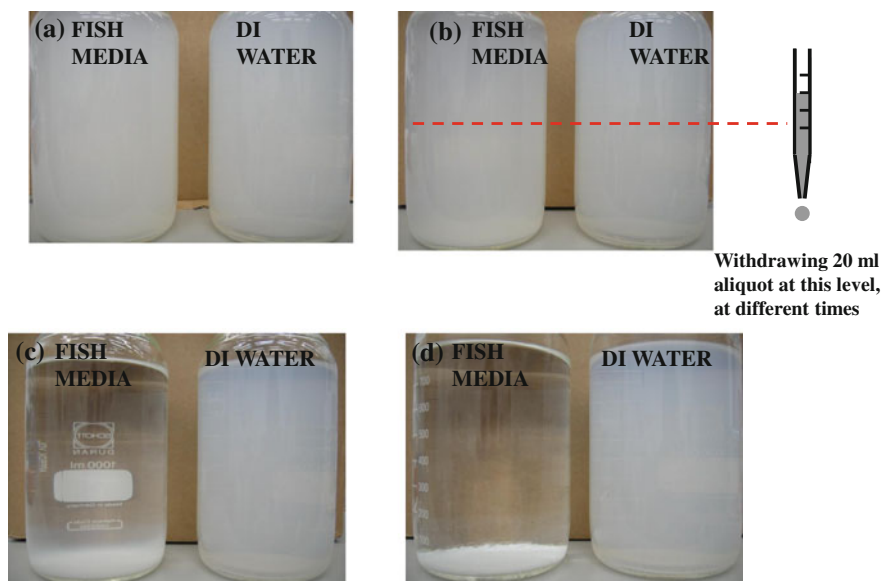
At various time intervals after preparing the dispersion, an aliquot of 25 mL was taken from a specific location, viz.: half way down the individual bottle (as illustrated in Fig. 1). To minimise disturbance of the dispersion the 25 mL aliquot was withdrawn gently using a pipette. The 25 mL was further sub-sampled into four 5 mL aliquots for the various analysis techniques. To minimise any variations in the nanoparticle dispersion within the sub-sampled aliquots, all measurements (using the various tools) were performed simultaneously immediately after the sub-sampling step. The removal of a 25 mL aliquot, sample splitting and subsequent analysis was repeated nine times within a period of 3 days, viz.: at (1, 60, 120, 180, 240, 1440, 1680, 2880, 3180) min, after preparing the dispersion. Results obtained from dispersion in DI water were compared to those in the corresponding fish medium. Unless otherwise noted, all analyses were performed at the native particle concentration without dilution.

Instrumentation

Dynamic light scattering (DLS) and zeta-potential analysis

Hydrodynamic size and zeta-potential (i.e., electrophoretic mobility) measurements were obtained using

Fig. 1 CeO₂ (50 mg/L) dispersed in fish media versus DI water. Images of visual sedimentation studies after: **a** 1 min (*Day 1*), **b** 120 min (*Day 1*), **c** 1440 min (*Day 2*), after dispersion, **d** 3180 min (*Day 3*). Figure indicates location where aliquot (20 mL) was withdrawn for subsequent sub-sampling and analysis



a Zetasizer Nano ZS (Malvern Instruments, UK) equipped with a 633 nm laser. The reference standard (DTS1230, zeta-potential standard from Malvern) was used to qualify the performance of the instrument. DLS particle size and zeta-potential measurements involved filling of a disposable capillary cell (DTS1060, Malvern). Prior to their use, these cells were thoroughly cleaned with ethanol and de-ionised water, as recommended by the instrument vendor. For analysis, the individual cell was filled with the appropriate sample and flushed before re-filling; measurement was carried out on the second filling. The same sample in the same cell was used for both DLS and zeta-potential measurements; here, zeta-potential measurements were taken immediately after acquiring the DLS measurement. Malvern Instrument's Dispersion Technology software (Version 4.0) was used for data analysis. For particle size, it is the z-average diameter (the mean hydrodynamic diameter) that is reported and zeta-potential values were estimated from the measured electrophoretic mobility data using the Smoluchowski equation (Malvern Instruments Ltd.).

Spectroscopic methods

The optical properties of the nanoparticles in suspension were evaluated using absorbance and

fluorescence spectroscopy. Absorbance scans from (250 to 800) nm were performed on a Lambda 850 UV-Vis spectrometer running UV Winlab software [Version 5.1.5] (Perkin Elmer, Seer Green, UK) using a slit width of 2 nm and a scan rate of 50 nm/min. Samples were placed into standard 1 cm path length quartz cuvettes from Starna Scientific (Hainault, UK). For the reference channel of the spectrophotometer, a matched cell containing the corresponding dispersing media (with no nanoparticles) was used. The instrument wavelength calibration was calibrated using Holmium glass standards (UR-HG, Serial # 9392), from Starna Scientific.

Fluorescence measurements were performed using a LS55 Luminescence Spectrophotometer running FL Winlab (Perkin Elmer). Fluorescence emission was recorded from (500 to 700) nm, with an excitation wavelength of 390 nm; slit widths for the excitation and emission sources were set at 5 and 10 nm, respectively, and spectra acquired at a scan speed of 50 nm/min. Blank spectra of the diluent/solvent were recorded and, where significant, subtracted from the appropriate scans. Wavelength calibration was corrected relative to SRM 936a quinine sulphate from National Institute of Standards and Technology (Gaithersburg, MD, USA). For both absorbance and fluorescence measurements three replicate aliquots of nanoparticle test solution were measured for each subsample.

Nanoparticle tracking analysis (NTA)

NTA was performed using a model LM10 (Nano-sight, Amesbury, UK). The system uses a 638 nm wavelength laser focused into a 300 μ l sample; for all experiments, a 20 \times objective was used to collect the scattered light. Samples were injected into the optical cell using a syringe, and nanoparticles visible within the field of view were individually tracked on a frame-by-frame basis using a charge-coupled device detector (variable electronic shutter duration ranged from 20 μ s to 30 ms). The resulting output is thus a collection of images (containing 640 \times 480 pixels) captured for a movie typically encompassing from 1000 to 5000 frames with a frame rate of 60 frames/s. Measurements were performed three times on each sample under repeatability conditions. The tracking and analysis software (NTA 2.0) was used to acquire, record, and determine the particle size and number count information. Instrument performance was qualified using a NIST-traceable latex nanosphere size standard from Thermo Scientific (Fremont, CA, USA), having a certified size of 97 nm \pm 3 nm (standard deviation 4.6%). The mean size measured for this standard using the NTA device was 100.8 nm with a standard deviation of 2.66 nm (based on five replicate measurements).

Scanning electron microscopy (SEM)

SEM images were obtained using a Supra 40 field emission scanning electron microscope from Carl Zeiss (Welwyn Garden City, Hertfordshire, UK), in which the optimal spatial resolution of the microscope was a few nanometres. In-lens detector images were acquired at an accelerating voltage of 15 kV, a working distance of \approx 3 mm, and a tilt angle 0 $^\circ$. For the analysis of the 'as received' nanoparticle powder, a sample of the powder was sprinkled over a SEM carbon adhesive disc; one side of the carbon disc was placed securely on a metal stub, whilst the other side was exposed to the nanoparticle powder. Excess powder was removed by gently tapping the stub on its side until a light coating of powder on the surface became apparent.

Detailed protocols for sample preparation of nanoparticles dispersed in liquid media onto poly-L-lysine slides suitable for SEM analysis have been reported elsewhere [8], and the appropriateness of

this protocol was evaluated by using NIST-traceable 100 nm latex beads (negatively charged) (supplied by Agar Scientific, UK). In summary, the protocol involved the deposition of an appropriate liquid sample (1 ml) on to a poly-L-lysine coated microscope glass slide (purchased from Fisher Scientific, UK) and allowing it to incubate for a period of 5 min at room temperature (\approx 20 $^\circ$ C) before dipping in a beaker of water in order to remove unbound nanoparticles. Slides were then allowed to dry under ambient conditions for \approx 2 h before they were thinly sputtered with gold using an Edwards S150B sputter coater unit (BOC Edwards, UK). Sputtering was conducted under vacuum (0.7 mPa or \approx 7 mbar), whilst passing pure, dry argon into the coating chamber. Typical plate voltage and current were 1,200 V and 15 mA, respectively. The sputtering time was approximately 10 s, which resulted in an estimated gold thickness of not more than a few nanometres being deposited on top of the substrate.

Data analysis

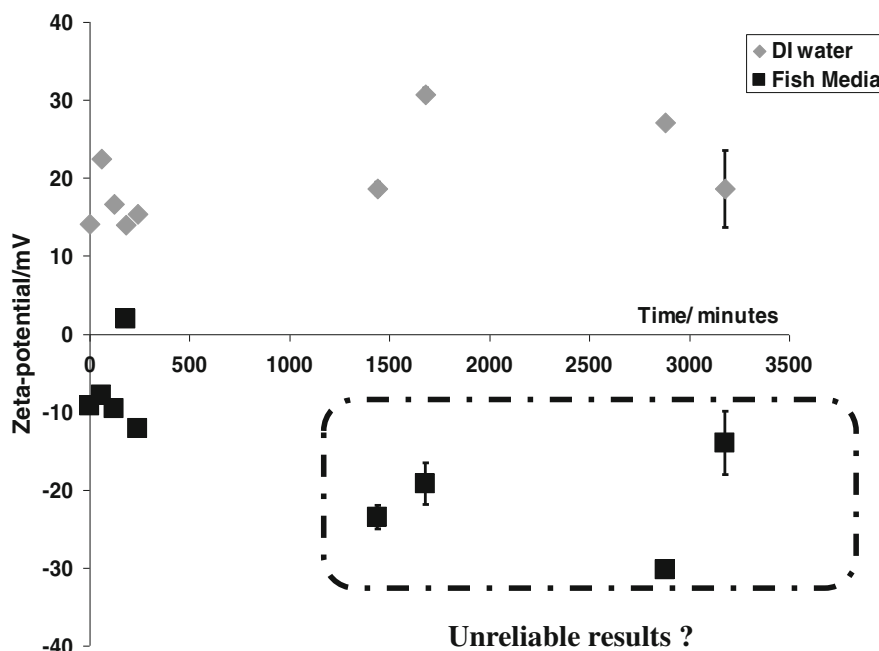
Data collected from all instruments (apart from SEM) were imported to a spreadsheet and the appropriate mean and standard deviations from the set of (three) replicates calculated. Results are plotted as mean values with error bars of one standard deviation i.e. the square root of the variance.

Results and discussion

Visual sedimentation and zeta potential

Figure 1 shows the results of a visual sedimentation experiment, when CeO₂ nanoparticles (50 mg/L) were dispersed in two separate media, DI water and fish medium, during the 3-day stability study. Results of this study show that on day 1, both bottles displayed roughly the same degree of turbidity, as represented by Fig. 1a and b (taken at 1 and 120 min, respectively). Although not apparent from the acquired images, there was evidence, upon careful examination of the bottles, that some particle sedimentation had occurred in both DI water and fish medium. By day 2 (1440 min after dispersion, Fig. 1c), there was clear proof that most of the particles have sedimented out in the fish medium,

Fig. 2 Zeta-potential of CeO₂ (50 mg/L) dispersed in fish media versus DI water, and sampled at various intervals during a 3-day dispersion stability study, with error bars of one standard deviation



whereas the DI water suspension is still visually turbid. By day 3, complete sedimentation had occurred in the fish medium (Fig. 3d).

In order to more fully understand the dispersion stability behaviour over time, zeta potential was monitored throughout the three-day study. Figure 2 shows the corresponding zeta-potential measurements for the particles dispersed in DI water and fish medium. The corresponding values shown in Fig. 2 are summarised in Table 2.

As shown in the plot, certain data points (of dispersions made in fish medium) are considered to be 'unreliable'; the reason being that the low particle concentrations resulted in low signal-to-noise and were flagged as unreliable by the instrument software quality report. The extremely low particle concentration in the later fish medium samples can also be observed from the corresponding visual sedimentation results in which the fluid sample under analysis became clear during the 3-day measurement period (Fig. 1d). However, even accepting a high degree of uncertainty in the magnitude of the measured zeta potential, the measured polarity (negative) of the particles is most likely correct. In both media, the reported zeta-potential values show some degree of variation: +14 to +31 mV (DI water, day 1–3) and +2 to –12 mV (for fish water, day 1 only).

More importantly, the zeta-potential values reported in Fig. 2 indicate an apparent charge reversal in going from DI water to fish medium. That is, particles dispersed in DI water exhibit a net positive charge, whereas particles in fish medium generally exhibit a net negative charge. The pH of DI water is slightly acidic (about pH 6), whereas the pH of the fish medium is close to neutral (pH 7.1 ± 0.1 over the entire experimental time frame). An IEP value of 8.1 ± 0.2 was determined by acidimetric titration of the CeO₂. Since the pH in both media is below the IEP, and should, therefore, support a positive net charge on the CeO₂ particles, the observed charge reversal suggests that one or more of the components in the fish medium are adsorbed on the CeO₂ particles causing a reduction in the IEP. A lower IEP would be consistent with development of a negative net charge in the fish medium at pH 7.1. This underscores the importance of measuring or knowing the pH, zeta potential and IEP for aqueous-based metal oxide nanoparticle systems where stability is being assessed.

The ionic composition of the fish medium includes both divalent metal cations (Ca²⁺ and Mg²⁺) and an oxyanion (sulphate, SO₄⁻), all of which have the potential to adsorb to oxide surfaces, and thus to shift the IEP (Hansmann and Anderson 1985). However, anionic sulphate, in particular, is known to bind

Table 2 Summary of zeta potential and corresponding s.d values (rounded off to 1 SF), as shown in Fig. 2

Time (min)	Zeta-potential			
	DI water (mV)	Standard deviation (mV)	Ecotox fish media (s.d.)	Standard deviation (mV)
1	14.1	0.3	-9.2	0.3
60	22.5	0.4	-7.8	0.6
120	16.7	0.2	-9.6	0.2
180	14.0	0.5	1.9	0.6
240	15.4	0.5	-12.1	0.3
1,440	18.6	0.8	-24	1
1,680	30.7	0.8	-19	3
2,880	27.1	0.4	-30.3	0.8
3,180	19	5	-14	4

strongly and to form surface complexes on CeO₂ nanocrystals (Xu et al. 2008), and thus is suspected as the principal agent in modifying the native IEP of CeO₂ in the fish medium. Specific adsorption of anionic species will shift the IEP in the acidic direction. The message made clear here is that the medium itself can modify the nanoparticle surface chemistry.

The rather unpredictable or fluctuating zeta-potential values for CeO₂ in both DI and fish water is a reflection of several factors, including the instability of the CeO₂ in an aqueous media, the nature of the zeta-potential measurement itself, and the changing particle concentrations in the fish medium; it is not due to changes in pH over time, as the pH remained within a narrow range from 7.0 to 7.2 throughout the duration of the experiment. With respect to CeO₂ stability, the rare earth oxides tend to be chemically unstable in water except under alkaline conditions, and hydrolysis–dissolution–precipitation reactions at the surface may occur that result in modification of the surface structure and chemistry (Baes and Mesmer 1976). However, zeta potential measurements can be inherently problematic with respect to reproducibility and are often subject to variation as observed in the present study; this is exacerbated by the low particle concentrations in the fish medium beginning on day 2.

In situ particle size results based on DLS

Figure 3a shows a time-dependent response of the mean particle size (*z*-average hydrodynamic diameter) when CeO₂ is dispersed in DI water versus fish

medium. The corresponding values shown in Fig. 3a are summarised in Table 3.

As before, data obtained from samples in the low concentration regime are deemed to be unreliable (i.e. in the case of fish medium on day 2–3) and will be excluded from the interpretation. Again, the poor reliability of the measurement was due to the low particle concentration of the sample under analysis; this was detected and reported by the software. Regardless, results show a substantial difference in mean particle size of CeO₂ in the two different media; particle size in DI water is ≈ 200 nm or less, whereas the particles are generally larger than 1 μ m in size in the fish medium. On day 1, fluctuations in particle diameter are already more apparent in the fish medium when compared to the corresponding DI water range (190–204 nm in DI water). The very large particle size differences observed between the two media are associated with the fact that large agglomerates of CeO₂ are found in the fish medium but not in DI water. An advantage of the DLS technique, in studies of agglomeration and aggregation, is that it is useful for the detection of small numbers of relatively large particles (i.e. in this case large agglomerates), due to the very strong intensity weighting. Furthermore, the presence of large particles can dominate the scattering when they are present at significant concentrations (Filipe et al. 2010).

The absolute accuracy of the DLS size results must be questioned, given the variations in particle concentration and the presence of large agglomerates; however, the trends are clear and unambiguous. It is

Fig. 3 DLS analysis of CeO₂ (50 mg/L) dispersed in fish media versus DI water, and sampled at various intervals during a three-day dispersion stability study: **a** mean hydrodynamic particle size; error bars of one standard deviation, **b** corresponding polydispersity index (PI)

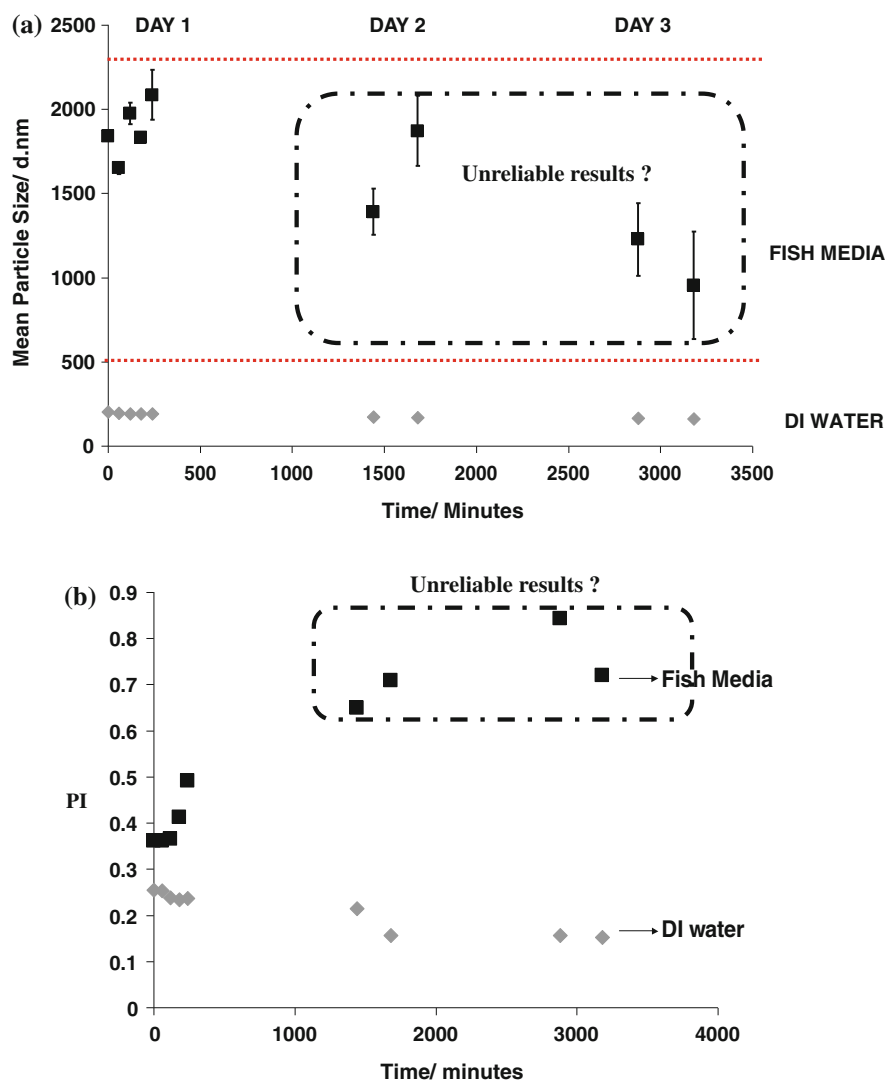


Table 3 Summary of DLS mean particle size and corresponding s.d values (rounded off to 1 SF), as shown in Fig. 3a

Time (min)	DLS mean particle size			
	DI water (d.nm)	Standard deviation (d.nm)	Ecotox fish media (d.nm)	Standard deviation (d.nm)
1	204	3	1,840	20
60	195	3	1,650	40
120	191	2	1,970	60
180	190	10	1,830	10
240	192	7	2,100	100
1,440	173	6	1,400	100
1,680	168	1	1,900	200
2,880	164	1	1,200	200
3,180	162	2	1,000	300

also clear that the mean particle size determined by DLS under the most stable conditions examined (i.e., in DI water on day 1), is significantly larger ($\approx 3\times$) than the median diameter reported by the vendor based on XDC analysis. This most likely reflects differences in the dispersion protocols used by the vendor and by the present authors. For instance, we did not attempt to optimise the stability conditions, and the vendor most likely would use the best possible dispersion condition and an optimised sample preparation approach for their analysis. Additionally, XDC is relatively less sensitive to low levels of undispersed aggregates, compared with the highly sensitive DLS technique.

Figure 3b shows the corresponding polydispersity index (PI) values, obtained from the cumulants analysis of DLS data. PI is a metric sensitive to the spread or polydispersity in the particle size distribution, and high values typically result when agglomerates form. For reasons previously given, the data associated with fish medium on days 2 and 3 are again marked as unreliable. Again, as in the mean particle size results (Fig. 3a), there is a clear distinction between the PI values in fish medium and DI water. From day 1, the PI values are observed to be larger in the fish medium compared to DI water; this suggests a broader particle size distribution in the fish medium when compared to DI water. In addition, on day 1, a much larger range of PI values are associated with the fish medium (0.36–0.49) as compared to DI water (0.26–0.23); the PI parameter (2nd moment) is typically less robust than the size parameter (1st moment) derived from the cumulants analysis. Interestingly, in the case of DI water, the PI value decreases with respect to time, from 0.255 (1 min on day 1) to 0.152 (3,180 min on day 3). This suggests that particle size distributions in DI water become narrower over the time-course of the experiment. But in reality this simply reflects the fact that larger agglomerates present in the water column on day 1 are gradually removed by sedimentation over time and their contribution to the DLS measurement therefore diminishes; it does not imply that larger particles are decreasing in size. Overall, the much broader particle size distribution implied by the larger PI value observed in the case of fish medium, is clearly related to the formation of agglomerates, a process that is absent in the case of DI water.

Analysis using NTA and SEM

Figure 4a shows the mean particle diameter of CeO₂ dispersed in DI water and fish medium, as acquired using the NTA method. The corresponding values shown in Fig. 4 are summarised in Table 4.

In contrast to findings from visual inspection and DLS measurements (as detailed above), the NTA particle size evaluation shows no distinction between the two media. Throughout the 3 days, variation in the particle diameter obtained in DI water (134–187 nm) is slightly lower than in fish medium (105–220 nm). Overall, when compared to the particle size reported by the DLS method (Fig. 3a), the NTA method yields a smaller particle size for a given sample; for example on day 1 (at 1 min) the mean particle diameter reported by NTA is 134 versus 204 nm as reported by DLS. Results also show that there is only a single data point that is considered to be unreliable i.e. when in fish medium on day 3 (3,180 min). This datapoint is unreliable because of the lack of nanoparticles suitable for tracking at this concentration. In addition to size information, the NTA method directly counts particles within the microscope's field of view and thus reports number concentration (Gallego-Urrea et al. 2009). Figure 4b shows the particle number concentration of CeO₂ with respect to time in the two different media. The corresponding values shown in Fig. 4b are summarised in Table 5.

Unlike the particle size information reported by the NTA method (Fig. 4a), there is a clear distinction between particles dispersed in the two media; there is roughly a 4-fold higher particle concentration as seen by the NTA for DI water versus fish medium. For example, on day 1, the particle concentration in DI water is $18 \times 10^8 \text{ mL}^{-1}$, whereas in the corresponding fish medium the concentration is $4 \times 10^8 \text{ mL}^{-1}$. Interestingly, throughout the 3-day stability study, there is a decreasing particle concentration with respect to time observed for both media, i.e. both dispersions seem to exhibit particle concentration decay profiles, the half-life of nanoparticles in the fish medium being much shorter than their half-life in water. This may be expected due to the increased agglomeration rate in fish medium. The advantage of NTA is the provision of a quantitative number concentration for particles in the size range that

Fig. 4 NTA analysis of CeO_2 (50 mg/L) dispersed in fish media versus DI water, and sampled at various intervals during a three-day dispersion stability study: **a** mean particle size, **b** particle number concentration. Error bars of one standard deviation

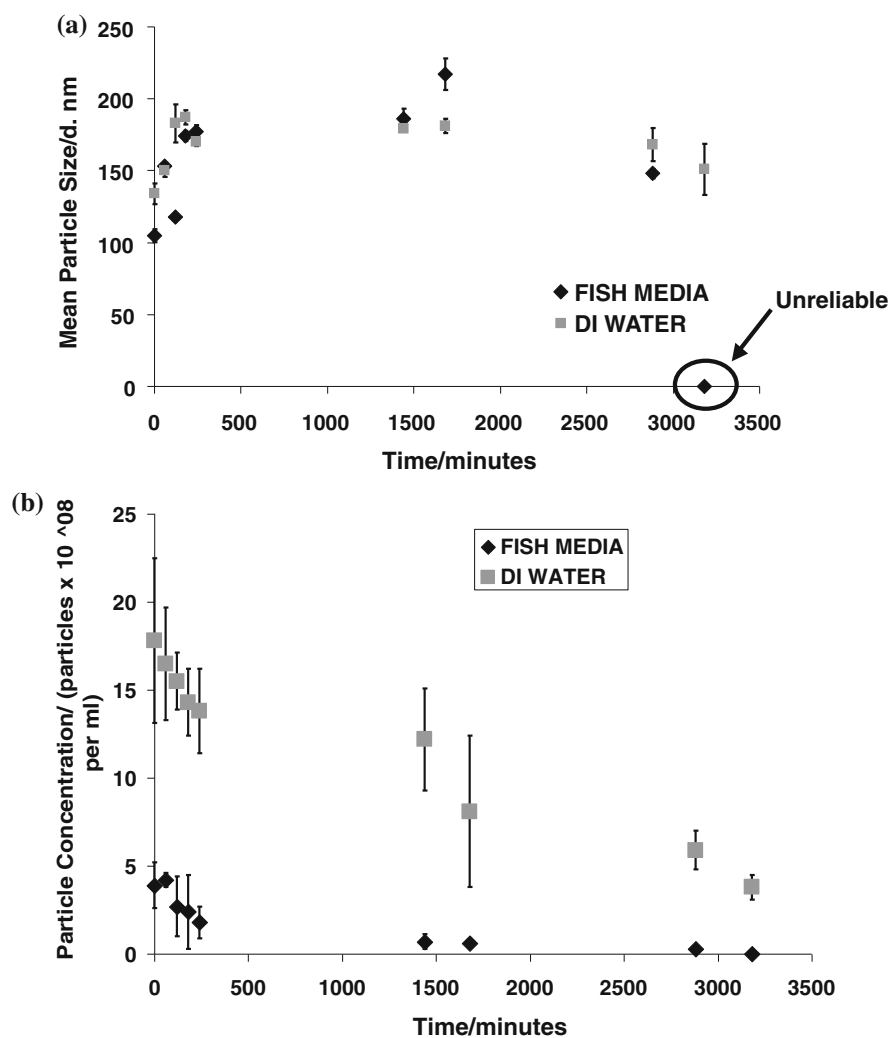


Table 4 Summary of NTA mean particle size and corresponding s.d. values (rounded off to 1 SF), shown in Fig. 4a

Time (min)	NTA mean particle size			
	DI water (d.nm)	Standard deviation (d.nm)	Ecotox fish media (d.nm)	Standard deviation (d.nm)
1	134	7	105	5
60	150	4	153	2
120	180	10	118	2
180	187	5	174	3
240	170	3	177	5
1,440	179	2	186	7
1,680	181	5	220	10
2,880	170	10	150	3
3,180	150	20	0	0

Table 5 Summary of NTA mean particle number concentration and corresponding s.d values (rounded off to 1 SF), as shown in Fig. 4b

Time (min)	Particle number concentration			
	DI water (particles \times 10^8 per mL)	Standard deviation (particles \times 10^8 per mL)	Ecotox fish media (particles \times 10^8 per mL)	Standard deviation (particles \times 10^8 per mL)
1	18	5	4	1
60	17	3	4.2	0.4
120	16	2	3	2
180	14	2	2	2
240	14	2	2	1
1,440	12	3	1	0
1,680	8	4	1	0
2,880	6	1	0	0
3,180	4	1	0	0

NTA can detect, however, it does not provide a simple indicator of agglomeration.

In general, particle size reported from DLS is larger than the particle size derived from the NTA method; for the fish medium, this difference is extremely large. The apparent inability of the NTA method to differentiate the state of the CeO₂ dispersion between the two different media, via particle size difference, can be attributed to several factors. Malloy and Carr (2006) have reported that the NTA method is not suitable for analysis of particles larger than about 600 nm and thus NTA is limited in that it is unable to track large agglomerates reliably. Firstly, the spot of light (arising from the light scatter of large particles) can become so large that its edges will vary between frames; this will mean that identifying its centre will become increasingly difficult, thus leading to centring errors, which are as large as the particle's movement. Secondly, large agglomerates will move too slowly to be reliably tracked and subsequently statistically underrepresented in the analysis.

The presence of large CeO₂ agglomerates in fish medium compared with their general absence in DI water was further verified using SEM analysis. Figure 5b and c shows representative SEM images of particles deposited from DI water and fish medium, respectively, on day 1 (120 min). The scale bar on both images is identical (200 nm). Results indicate that particles are generally more massive and fewer in number within the fish medium relative to DI water, as would be expected if the particles were unstable and agglomerating. In fish medium, the predominant particle size is greater than 2,000 nm (if estimated to

the dimension of a sphere); whereas, in DI water the particle size is estimated to be \approx 300 nm. Interestingly, also present in the fish medium are much smaller particles, i.e. under 250 nm; this is consistent with the NTA results. Figure 5a shows the corresponding 'as received' powder; it is clear that the highly aggregated and agglomerated material has been reduced to a much smaller particle size through the sonication process. The presence of large agglomerates observed in SEM images in the fish medium is consistent with the DLS results and sedimentation behaviour previously described.

UV-Vis spectroscopy and particle concentration

Figure 6a shows a typical UV-visible absorption spectrum (250–800 nm) for the CeO₂ dispersion in DI water obtained on day 1 (1 min); the spectrum displays a maximum at \approx 316 nm with a peak absorbance of 1.2. One of the advantages in UV-Vis spectroscopy is that it can provide a direct measure of absolute concentration, as governed by the Beer-Lambert law (Pavia et al. 2008); this law is often associated with the measurement of dissolved analyte rather than particles in suspension. Hence, if light is scattered from particles in the light path, then this may lead to deviations from the Beer-Lambert law and thus will affect the reliability of the estimated concentration. In an attempt to calibrate the UV-Vis spectrometer, the CeO₂ absorbance (at λ_{\max}) was recorded against nanoparticle concentration, as shown in Fig. 6b. These results were obtained by preparing a concentrated stock dispersion in DI water and diluting

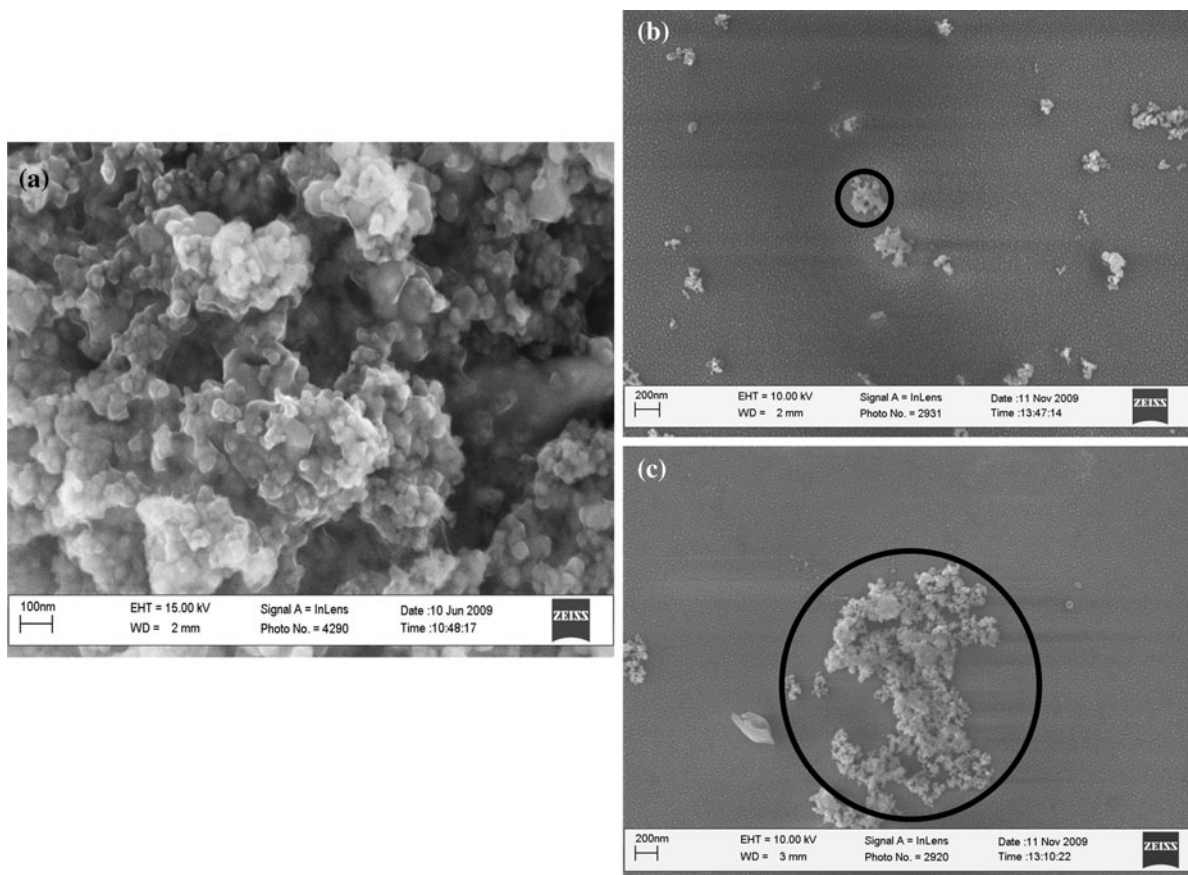


Fig. 5 SEM images of CeO_2 (50 mg/L): **a** as-received powders, **b** dispersed in DI water at 120 min (Day 1 of the stability study), **c** dispersed in fish media at 120 min (Day 1 of the stability study)

appropriately, so as to result in the desired CeO_2 concentrations; the UV–Vis data were acquired and the corresponding peak intensity at peak maximum obtained.

Results show that the concentration of particles can be linearly correlated to the measured absorbance (up to a concentration of 100 mg/L); data-sets above this concentration range do not follow this linear relationship. If the y -intercept in the dataset is forced to zero (as predicted by the Beer–Lambert law), then the plot loses its linearity. Deviations from this law can be due to the fact that particles are scattering as well as absorbing in nature and it would be very difficult to estimate the degree of scattering relative to absorbance. Thus, empirically it can be argued that the absorbance reading reported here should be thought of as ‘apparent absorbance’ uncorrected for scattering and other non-linear effects. Additionally, this calibration curve will likely change if the

agglomeration state changes substantially, since this will greatly impact the scattering properties.

Figure 6c shows a plot of the UV–Vis intensity at λ_{max} versus time for CeO_2 dispersed in the two media. Overall, results show that there is sufficient difference in the intensity response in the two media. The trends expressed in Fig. 6c are consistent with the visual inspection of the test suspensions as discussed previously. For example, on day 1 (at 1 min), absorbance intensity is 1.3 when in DI water but is 0.7 when in fish medium. From comparison of the two plots, it is apparent that the particle concentration in the fish medium decays much more rapidly compared to DI water. In the case of fish medium, experiment time from (1–240) min, shows that intensity at λ_{max} decreases from (0.7–0.3) a.u. after which the apparent concentration begins to level off and eventually reaches a low but fairly stable level. This is clearly different in

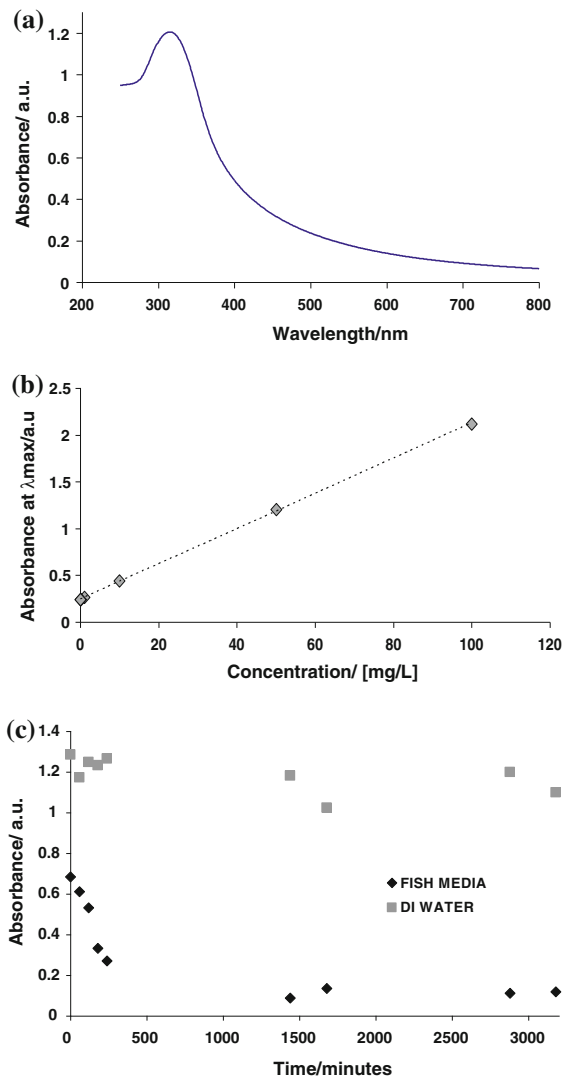


Fig. 6 Optical absorbance of CeO₂: **a** spectrum when dispersed in DI water (50 mg/L) taken at 1 min, **b** calibration curve for absorbance versus CeO₂ concentration, used to confirm the applicability of the Beer–Lambert law, **c** comparison of optical absorbance at the wavelength of maximum absorbance in fish media (at 325 nm) versus DI water (at 312 nm) over time (during 3-day stability study), at 50 mg/L CeO₂

the case of DI water, in which the apparent particle concentration is more or less stable over the initial 240 min, followed by a slight reduction towards a plateau level well above that observed in the fish medium. The rapid initial decay of the apparent particle concentration in the fish medium suggests that the agglomeration events mainly occurred on day 1, with most of the particles sedimenting out by day 2

(this observation correlates well with the visual sedimentation experiment as shown in Fig. 1c).

Interestingly, we have observed that there is a shift in the λ_{max} value for absorbance when particles are dispersed in DI water versus fish medium; i.e., 312 versus 325 nm, respectively. Past researchers have attributed this red shift to an increase in particle size (Nguyen et al. 2009).

Fluorescence spectroscopy

Figure 7a, depicts a typical fluorescence spectrum (excitation of 390 nm, spectral range from 500 to 700 nm) of CeO₂ in DI water. The spectrum here shows a peak maximum at 553 nm with fluorescence intensity of 296. In addition, errors due to scattering effects of the nanomaterial will exist, just as in UV–Vis spectroscopy. Figure 7b shows how the intensity at λ_{max} (553 nm) changes with respect to time over the period of the experiment. The results track very closely with UV–Vis absorbance. Again, we are able to differentiate between particles dispersed in fish medium and those dispersed in DI water; for example on day 1 (1 min), fluorescence intensity is 319 versus 267 a.u., for DI water and fish medium, respectively. Again, the DI water profile shows a stable response, in which the signal ranges from (319 to 292) a.u. The fish medium intensity signal on the other hand decays rapidly on the first day before it levels off on Day 2. As in the UV–Vis results, the decay profile that is observed for the fish medium is consistent with the continual decrease in particle concentration over time.

In contrast to the UV–Vis absorbance peak wavelength, the peak emission wavelength was identical in both dispersion media; also it did not change with respect to time in the different media.

Summary of techniques to assess dispersion stability

In the context of ecotoxicology, the premise of the present work was that different measurement techniques have the potential to yield complementary information with regards to assessing nanoparticle dispersion stability. In the present study, stability was evaluated over the course of 3 days for the dispersion of nanocrystalline CeO₂ in DI water and fish medium using the following approaches:

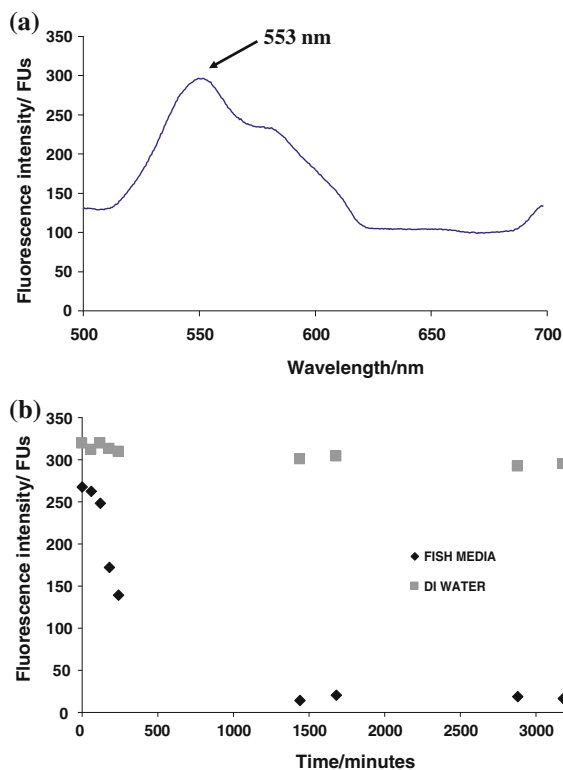


Fig. 7 Fluorescence response of CeO₂ (50 mg/L): **a** spectrum when dispersed in DI water obtained at 1 min, **b** comparison of fluorescence intensity (at maximum emission wavelength of 553 nm) in fish media versus DI water as a function of time (during 3-day stability study)

1. Assessing changes in particle size with time The DLS technique, which yields particle size and PI, was shown to be extremely sensitive in monitoring the onset of agglomeration. Although DLS can monitor the onset and progression of agglomeration leading to the formation of large agglomerates, care must be taken in evaluating and reporting absolute values of particle size derived from DLS. Firstly, the technique reports an equivalent spherical hydrodynamic diameter that is impacted by factors such as surface charge, adsorption of molecular species from solution and morphology or shape (Murdock et al. 2008). Secondly, DLS is sensitive to the presence of small numbers of large particles within the sample, such as agglomerates; results are heavily weighted toward the larger size particles due to the strong dependence of scattered intensity on size (Le et al. 2008). In contrast, the NTA method provides a number-weighted hydrodynamic size, and thus does not have the overt sensitivity to larger size particles. However,

for the conditions of the present study NTA proved to be ill-suited for monitoring agglomeration, as results show that it was only able to differentiate between two distinctly different stability regimes represented by the DI water and fish medium by the vanishing concentration of nanoparticles in the latter case. Such an observation on its own would be unable to distinguish, for example, dissolution from agglomeration.

Of the two spectroscopic-based techniques used in this study, only UV–Vis spectroscopy was shown to have measurable sensitivity to changes in particle size for nanocrystalline CeO₂, via a shift in the wavelength of the maximum absorbance peak. Fluorescence spectroscopy did not exhibit such a dependency.

2. Sedimentation rate through particle concentration measurement Several techniques offer methods for sensing changes in particle concentration resulting from sedimentation of larger agglomerates in unstable suspensions, including NTA, UV–Vis absorption and fluorescence emission. Overall, the sensitivity is greatest for the spectroscopic methods based on the relative change in signal as a function of time. But, whereas NTA offers quantitative particle counting, the spectroscopic methods require calibration and are subject to nonlinear effects that likely alter with changes in agglomerate size. Visual sedimentation experiments are useful as it gives a direct observation of sedimentation events, allowing researchers to quickly and easily assess relative dispersion stability. Although not used in the present study, turbidimetry is a simple inexpensive concentration sensitive method that essentially quantifies what we have observed visually: i.e., the reduction of scattering due to loss of particles during sedimentation (Kissa 1999).

3. Surface chemistry and electrokinetics Measurement of zeta potential (note: in actuality, the particle electrophoretic mobility is determined by Doppler light scattering, which is then converted to zeta potential using a theoretical model) is the only example employed from this group of surface-related techniques in the present study. Zeta potential is the most conveniently measured parameter that is sensitive to particle surface charge; surface charge properties are directly relatable to colloidal stability in electrostatically stabilized systems, and play a significant role in determining how nanoparticles

interact with their environment (Jailani et al. 2008). However, zeta-potential results should be interpreted and reported with care, since they are sensitive to trace contamination by surfactants and certain other ionic species and are inherently model-dependent. Zeta potential is most reliable when assessing the polarity of particle charge, tracking relative changes in particle surface charge behaviour, and quantifying the acid–base properties of the particle surface via determination of the IEP (Hang et al. 2009); zeta-potential results generally should not be considered absolute or quantitative unless great care is taken to ensure the integrity of the measurement and the appropriate selection of the model used to convert mobility to zeta potential. In the present study, results indicate a charge reversal in comparing particles dispersed in DI water versus fish medium, with much lower absolute zeta-potential values in fish medium during the first few hours after dispersion relative to DI water; the charge reversal was attributed to adsorption of sulphate ions from the fish medium. The fact that zeta potential remained between about +15 and +30 mV in DI water throughout the 3-day study may help explain why this dispersion is more stable than one prepared in fish medium.

Conclusions

In summary, the above techniques show that if dispersion stability is measured by monitoring the:

- (a) presence of agglomerates through changes in particle size: then DLS appears optimally sensitive, whilst UV–Vis absorbance may be suitable though far less sensitive and certainly material dependent,
- (b) particle sedimentation: then NTA, UV–Vis absorbance or fluorescence emission are all suitable, with NTA perhaps yielding more quantitative results. The suitability of the spectroscopic methods will be highly material dependent, and may work better for some nanoparticles than others,
- (c) surface charge: then zeta potential derived from electrophoretic mobility measurements is probably the most accessible and relevant parameter for dilute nanoparticle suspensions; electro-acoustic methods are more suitable for high

solids loadings where optical properties do not permit the use of laser light scattering electrophoresis.

Acknowledgments This work was conducted as part of PROSPeCT, which is a public–private partnership between DEFRA, EPSRC and TSB and the Nanotechnology Industries Association (NIA Ltd.) and its members, and was administered by the DEFRA LINK Programme. Authors would like to thank Drs. Neil Harrison, Andrew Shaw and Alex Shard for useful discussions and continuing support and Mr. Jordan Tompkins for the initial handling and distribution of the nanomaterials. We acknowledge the use of instruments in the Biotechnology and Materials groups at NPL.

References

- Baes CFJ, Mesmer RE (1976) *The hydrolysis of cations*. Wiley, New York
- Boverhof DR, David RM (2010) Nanomaterial characterization: considerations and needs for hazard assessment and safety evaluation. *Anal Bioanal Chem* 396(3):953–961
- Filipe V, Hawe A, Jiskoot W (2010) Critical evaluation of nanoparticle tracking analysis (NTA) by NanoSight for the measurement of nanoparticles and protein aggregates. *Pharm Res* 27(5):796–810
- Gallego-Urrea JA, Tuoriniemi J, Pallander T, Hasselov M (2009) Measurements of nanoparticle number concentrations and size distributions in contrasting aquatic environments using nanoparticle tracking analysis. *Environ Chem* 7(1):67–81
- Handy RD, von der Kammer F, Lead JR, Hasselov M, Owen R, Crane M (2008) The ecotoxicology and chemistry of manufactured nanoparticles. *Ecotoxicology* 17(4):287–314
- Hang JZ, Shi LY, Feng X, Xiao L (2009) Electrostatic and electrosteric stabilization of aqueous suspensions of barite nanoparticles. *Powder Technol* 192(2):166–170
- Hansmann DD, Anderson MA (1985) Using electrophoresis in modeling sulfate, selenite, and phosphate adsorption onto goethite. *Environ Sci Technol* 19(6):544–551
- ISO 7346-3 (1996), *Water quality—Determination of the acute lethal toxicity of substances to a freshwater fish, Part 3: Flow-through method*. ISO, Geneva
- Jailani S, Franks GV, Healy TW (2008) Zeta-potential of nanoparticle suspensions: effect of electrolyte concentration, particle size, and volume fraction. *J Am Ceram Soc* 91(4):1141–1147
- Kissa EE (1999) *Dispersions: characterization testing and measurement*. CRC Press, Boca Raton, USA
- Le TT, Saveyn P, Hoa HD, der Meeren PV (2008) Determination of heat-induced effects on the particle size distribution of casein micelles by dynamic light scattering and nanoparticle tracking analysis. *Int Dairy J* 18(12):1090–1096
- Malloy A, Carr B (2006) Nanoparticle tracking analysis—The halo (TM) system. *Part Part Syst Charact* 23(2):197–204

- Malvern Instruments Ltd. Technical information provided for the Zeta-sizer Nano. <http://www.malvern.com/zetasizer>
- Murdock RC, Braydich-Stolle L, Schrand AM, Schlager JJ, Hussain SM (2008) Characterization of nanomaterial dispersion in solution prior to In vitro exposure using dynamic light scattering technique. *Toxicol Sci* 101(2):239–253
- Nguyen DT, Kim DJ, Myoung GS, Kim KS (2009) Experimental measurements of gold nanoparticle nucleation and growth by citrate reduction of HAuCl₄. *Adv Powder Technol* 21(2):111–118
- Pavia DL, Lampman GM, Kriz GS, Vyvyan JA (2008) Introduction to spectroscopy, 4th edn. Brooks Cole, Belmont, USA
- Powers KW, Brown SC, Krishna VB, Wasdo SC, Moudgil BM, Roberts SM (2006) Research strategies for safety evaluation of nanomaterials. Part VI. Characterization of nanoscale particles for toxicological evaluation. *Toxicol Sci* 90(2):296–303
- Reference Material 8012—Gold nanoparticles, Report of investigation, National Institute of Standards and Technology, U.S. Department of Commerce, https://www-s.nist.gov/srmors/view_detail.cfm?srm=8012
- Simonet BM, Valcarcel M (2009) Monitoring nanoparticles in the environment. *Anal Bioanal Chem* 393:17–21
- Tantra R, Jing S, Gohil D (2010) Section 4: New trends in environmental toxicology. “Technical issues surrounding the preparation, characterization and testing of nanoparticles for ecotoxicological studies”. In Popov V, Brebbia CA (eds) *Environmental toxicology 3*. WIT Press, Southampton, vol 132, pp 165–176
- Tiede K, Boxall ABA, Tear SP, Lewis J, David H, Hasselhoff M (2008) Detection and characterization of engineered nanoparticles in food and the environment. *Food Addit Contam* 25(7):795–821
- Xu J, Li G, Liping L (2008) CeO₂ nanocrystals: seed-mediated synthesis and size control. *Mater Res Bull* 43(4):990–995